

OPTIMAL SHORTENING VELOCITY (V/V_{\max}) OF SKELETAL MUSCLE DURING CYCLICAL CONTRACTIONS: LENGTH–FORCE EFFECTS AND VELOCITY-DEPENDENT ACTIVATION AND DEACTIVATION

GRAHAM N. ASKEW* AND RICHARD L. MARSH

Department of Biology, Northeastern University, 360 Huntington Avenue, Boston, MA 02115, USA

*Present address: Department of Zoology, University of Cambridge, Downing Street, Cambridge CB2 3EJ (e-mail: gna22@cam.ac.uk)

Accepted 18 February; published on WWW 27 April 1998

Summary

The force–velocity relationship has frequently been used to predict the shortening velocity that muscles should use to generate maximal net power output. Such predictions ignore other well-characterized intrinsic properties of the muscle, such as the length–force relationship and the kinetics of activation and deactivation (relaxation). We examined the effects of relative shortening velocity on the maximum net power output (over the entire cycle) of mouse soleus muscle, using sawtooth strain trajectories over a range of cycle frequencies. The strain trajectory was varied such that the proportion of the cycle spent shortening was 25, 50 or 75 % of the total cycle duration.

A peak isotonic power output of 167 W kg^{-1} was obtained at a relative shortening velocity (V/V_{\max}) of 0.22. Over the range of cyclical contractions studied, the optimal V/V_{\max} for power production ranged almost fourfold from 0.075 to 0.30, with a maximum net power output of 94 W kg^{-1} . The net power output increased as the proportion of the cycle spent shortening increased. Under conditions where the strain amplitude was high (i.e. low cycle frequencies and strain trajectories where the proportion of time spent shortening was greater than that spent lengthening), the

effects of the length–force relationship reduced the optimal V/V_{\max} below that predicted from the force–velocity curve. At high cycle frequencies and also for strain trajectories with brief shortening periods, higher rates of activation and deactivation with increased strain rate shifted the optimal V/V_{\max} above that predicted from the force–velocity relationship. Thus, the force–velocity relationship alone does not accurately predict the optimal V/V_{\max} for maximum power production in muscles that operate over a wide range of conditions (e.g. red muscle of fish).

The change in the rates of activation and deactivation with increasing velocity of stretch and shortening, respectively, made it difficult to model force accurately on the basis of the force–velocity and length–force relationships and isometric activation and deactivation kinetics. The discrepancies between the modelled and measured forces were largest at high cycle frequencies.

Key words: muscle mechanics, skeletal muscle, power output, shortening velocity, model, velocity-dependent activation, velocity-dependent deactivation, stretch, length, force, mouse.

Introduction

The muscular generation of power is required by animals (including humans) during one-shot events, such as throwing and jumping, and during repetitive activities such as flying, swimming, cycling and rowing. How much power muscles are able to produce may limit the performance of such movements. The maximum net power output of muscle (over complete cycles of lengthening and shortening) is determined by its intrinsic properties: the isometric stress, the force–velocity relationship and the kinetics of activation and deactivation (Josephson, 1993). These properties of muscle are readily measured *in vitro*, enabling predictions about the *in vivo* function of muscle to be made. However, the conditions under which the basic properties are measured influence the results and make predictions about *in vivo* conditions more difficult.

A muscle generates work by shortening whilst it exerts a force. The mechanical power output is defined as the rate of

doing work and is equal to the product of force and shortening velocity. The force that a muscle can generate is dependent on the rate at which it shortens, force (P) being inversely related to shortening velocity (V). This association is described as the force–velocity relationship and is illustrated in Fig. 1A. The muscle generates its maximum force (P_0) when it is held isometric and shortens at its maximum rate (V_{\max}) when the load is zero. Consequently, the isotonic power output is zero at P_0 and V_{\max} and is maximal at intermediate forces and velocities (Fig. 1C,D). For example, typical V/V_{\max} and P/P_0 values at which maximum isotonic power output is generated in mouse muscles are 0.22 and 0.38, respectively, for soleus and 0.26 and 0.44, respectively, for the extensor digitorum longus (EDL) (Fig. 1; Askew and Marsh, 1997). It has been suggested that power-generating muscles should operate, during natural activities, at shortening velocities corresponding

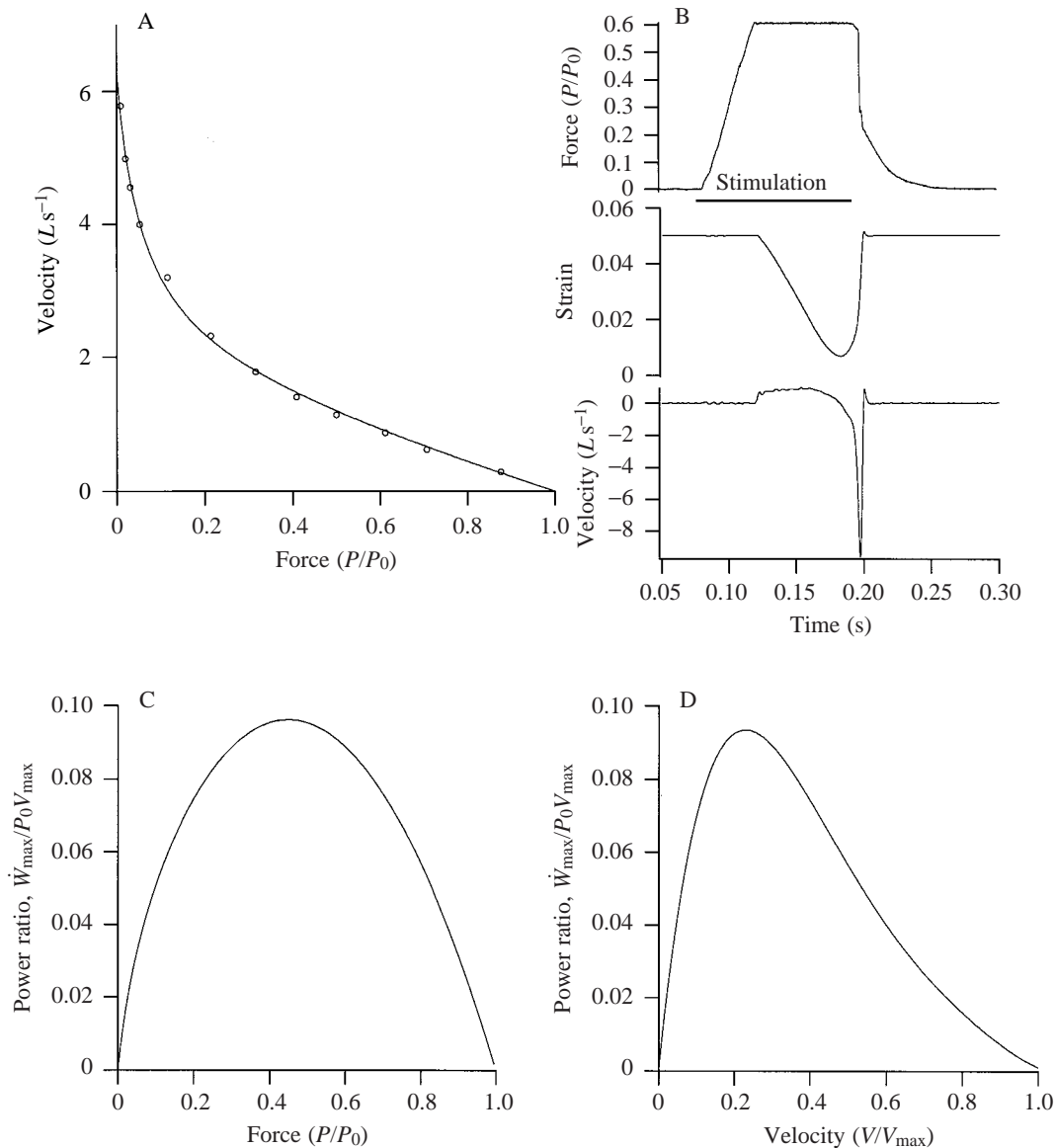


Fig. 1. (A) Illustration of the isotonic force–velocity relationship of a typical mouse soleus muscle, determined using after-loaded shortening contractions. A hyperbolic–linear equation has been fitted to the data (Marsh and Bennett, 1986). (B) Force, strain and velocity records from a muscle shortening during an isotonic contraction. The muscle shortens whilst force is ‘clamped’, allowing the peak shortening velocity to be determined by differentiating strain with respect to time. (C,D) Peak power expressed as a power ratio ($\dot{W}_{max}/P_0 V_{max}$), where \dot{W}_{max} is the maximum isotonic power output, corresponds to a force of $0.45P_0$ (C) and a velocity of $0.23V_{max}$ (D). The data presented are for a muscle with a mass of 4.3 mg, a fibre length of 8.7 mm, a maximum shortening velocity V_{max} of $6.28 L s^{-1}$, where L is muscle length, and a peak isometric stress P_0 of $271 kN m^{-2}$. Force is expressed relative to maximum isometric stress P_0 .

to those that yield maximum power output during isovelocity contractions (Hill, 1950; Goldspink, 1977; Rome, 1994; Lutz and Rome, 1996). Comparisons of *in vivo* shortening velocities with force–velocity curves determined *in vitro* indicate that some muscles operate at V/V_{max} ratios close to those that yield peak power output from the force–velocity curve. For example, during fish swimming, the active fibres shorten at a V/V_{max} that corresponds to a value producing approximately peak isotonic power output on the basis of the force–velocity curve (Rome *et al.* 1988, 1992; Rome, 1994). Lutz and Rome (1996)

concluded that the muscles in jumping frogs also shorten at a similarly optimal V/V_{max} , but other data suggest that this conclusion may not apply to all muscles used in jumping (Marsh, 1994).

In the present investigation, the effects of cycle frequency and strain trajectory on the optimal V/V_{max} for maximum net power output in mouse soleus muscle were examined. We hypothesized that factors in addition to the force–velocity relationship, such as the length–force relationship and changes in the kinetics of activation and deactivation, would produce a shift in the optimal

V/V_{\max} under different conditions. The mouse soleus muscle was selected for these experiments as it provides a convenient model in which the effects of V/V_{\max} on power output can be examined. We used sawtooth cycles in which velocity was held constant during most of the shortening and lengthening periods. Such cycle shapes are realistic for some muscles (Girgenrath and Marsh, 1997); however, we do not suggest that any of the experimental protocols used here reflect the conditions under which the soleus muscle is used in the mouse.

Materials and methods

Female white mice (ICR, Taconic) aged between 4 and 7 weeks were killed by cervical dislocation. The skin was removed from the hind limbs, which were subsequently removed at the hip and placed in oxygenated Ringer's solution at room temperature (approximately 23 °C). The composition of the Ringer (in mmol l⁻¹) was: NaCl, 144; sodium pyruvate, 10; KCl, 6; MgCl₂, 1; NaH₂PO₄, 1; MgSO₄, 1; Hepes, 10; CaCl₂, 2; pH 7.4 at room temperature, adjusted using Trizma base (after Daut and Elzinga, 1989). The soleus muscle from each leg was carefully dissected out, and small aluminium foil clips (Ford *et al.* 1977) were attached to the distal tendons as closely as possible to the fibres without causing damage. One muscle was used immediately, whilst the other was left pinned out in a Petri dish in oxygenated Ringer at room temperature, at approximately its resting length.

The same arrangement was used throughout the experiments. The muscle was suspended vertically in a Perspex, flow-through experimental chamber, circulated with oxygenated Ringer's solution at 37 °C. The proximal tendon was secured to the base of the experimental chamber using a stainless-steel clip. The aluminium clip on the distal tendon was used to attach the muscle to the lever of an ergometer (Cambridge Technology Inc., series 300B) *via* a lightweight silver chain. The ergometer was mounted on a stage that could be raised and lowered above the experimental chamber using a fine vertical adjustment, allowing the muscle's length to be adjusted in increments of 0.01 mm. The initial length of the muscle was set to approximately resting length, and a period of approximately 30 min was allowed for recovery from the dissection and for thermoequilibration.

Isometric properties and optimization of starting length

Following the recovery period, the length of the muscle was adjusted to that yielding the maximum twitch force using a series of isometric twitches (L_{tw}). The muscle was stimulated using a pair of parallel platinum electrodes, which ran the full length of the muscle to ensure uniform activation. Supramaximal stimuli, with a pulse width of 0.25 ms, were amplified using a direct current amplifier and delivered to the muscle. The optimum length of the muscle for the production of isometric tetani was determined using a series of fused tetani (stimulation frequency 150 Hz) and was defined as L_0 . This length was used in the cyclical work studies, having been found previously to correspond to the optimum length for work

production (Askew and Marsh, 1997). Typically, L_0 was approximately 7 % less than L_{tw} .

Isometric twitches were characterized by measuring the latency of activation, time to half-peak force, time to peak force, time from peak force to half-relaxation and time to 90 % relaxation at L_{tw} . Tetani were characterized by measuring the time to half-force from the last stimulus, at L_0 . A period of 1 min was allowed between each twitch, and 5 min was allowed between each tetanus for metabolic recovery. The maximum isometric tetanic force (P_0), the mean fibre length ($L_f=0.85L_0$; Askew and Marsh, 1997), the wet mass (determined at the end of the experiment using an electronic balance, having blotted off excess Ringer's solution using filter paper) and the density of muscle (1060 kg m⁻³; Méndez and Keys, 1960) were used to calculate the maximum isometric stress.

Force-velocity properties

The force-velocity properties of the first muscle were determined using after-loaded isotonic tetanic contractions, illustrated in Fig. 1. The starting length of the muscle was set to 5 % above L_0 such that, when the muscle shortened, the shortening took place across the plateau region of the length-force relationship. The muscle was tetanically stimulated at the fusion frequency of the muscle, allowing force to rise to a predetermined level. The force was 'clamped' and the muscle allowed to shorten (Fig. 1B). Force and length signals were amplified (model LPF-202, Warner Instruments, Corp.) and recorded using a 12-bit A/D converter with a sampling frequency of 5 kHz. Muscle length was converted to muscle strain (muscle length - L_0)/ L_0 . The strain trace was differentiated with respect to time, and the peak shortening velocity was measured. Fig. 1B shows force, strain and velocity traces for a typical contraction. The process was repeated for loads ranging from approximately 0.90 P_0 to 0.01 P_0 , allowing 5 min between each contraction for metabolic recovery. An isometric tetanus was performed at L_0 between every four isotonic measurements, allowing correction for any decline in muscle performance. Velocity was plotted against the corrected force, and a hyperbolic-linear curve was fitted to the data (Marsh and Bennett, 1986) using the non-linear curve-fitting procedures in the application Igor (Version 3.0, WaveMetrics), allowing the maximum velocity of shortening (V_{\max}) to be estimated by extrapolation to zero force.

Cyclical contractions at different V/V_{\max}

The second muscle was used to measure the mechanical power output during cyclical contractions. Initially, the starting length of the muscle was set to L_0 using a series of isometric tetani, as described above. The work loop technique (Josephson, 1985) was used to impose cyclical length changes upon the muscle whilst it was phasically stimulated. The ergometer controlled the length of the muscle using a computer-generated wave in the application SuperScope II (Version 2.1) which was converted into an analogue signal by a 16-bit A/D converter. A stimulation wave was synchronized to the length wave, but could be offset by using a phase shift. Force and length outputs were

amplified (LPF-202, Warner Instruments, Corp.) and recorded on a Macintosh IIfx computer using a 12-bit A/D converter with a sampling frequency of 5 kHz. The muscle was subjected to five cycles of work at 5 and 9 Hz, but to only two cycles at 1 Hz to limit fatigue. The instantaneous power output of the muscle was calculated as the product of force and velocity; the net power output was the instantaneous power output averaged over the whole cycle, using an average of the work generated in loops 3–5 (work generated in the first loop was used at low cycle frequencies). The net work performed was the product of net power output and cycle duration (frequency⁻¹). Work loops were generated by plotting force against strain.

Initially, a series of four control work loops was performed at a cycle frequency of 5 Hz. These were carried out using a sinusoidal length trajectory and an optimal phase, stimulation duration and strain amplitude for maximizing work production (typically: phase 11 ms before the start of shortening, stimulation duration 65–70 ms, i.e. 10 or 11 stimuli at 150 Hz, strain amplitude $\pm 6\%$ of L_0). A period of approximately 5 min was allowed between each set of work loops for metabolic recovery. Control loops were carried out throughout the course of the experiment (usually every five or six runs, but after every run at low frequencies) in order to monitor any decline in the muscle's performance. Any decline was corrected by assuming a linear decline between consecutive controls. The experimental run was terminated if the muscle's control power output fell below 80% of the initial measurement.

Cycle frequencies of 1, 5 and 9 Hz were investigated, and three different length trajectories were imposed on the muscle at each frequency: saw25% (sawtooth strain with 25% of the cycle spent shortening and 75% of the cycle lengthening), saw50% and saw75% (abbreviated using similar terminology; see Askew and Marsh, 1997). For each combination of frequency and length trajectory, the phase and duration of stimulation were optimized to yield the maximum power output. The muscle strain amplitude (L_A) as a fraction of L_0 was selected which corresponded to a particular V/V_{\max} , using V_{\max} estimated from the first muscle and the following formula:

$$L_A = \frac{(V/V_{\max})V_{\max}S}{2f}, \quad (1)$$

where V/V_{\max} ranged from 0.025 to 0.4, V_{\max} is the maximum velocity of shortening estimated from the contralateral muscle (Ls^{-1} , where L is the resting length of the muscle), S is the proportion of the cycle spent shortening, and f is the cycle frequency. For example, for a V/V_{\max} of 0.2 at a cycle frequency of 5 Hz using a saw50% length trajectory, for a muscle with $V_{\max}=6.5 Ls^{-1}$, $L_A=\pm 0.065L_0$. Strain amplitudes exceeding $\pm 25\%$ of L_0 were not used to avoid damaging the muscle.

Results

Isometric and isotonic properties

All data are presented as mean \pm S.E.M. (N = number of replicates). The mice used in the experiments had a mean mass

of 23.8 ± 0.7 g ($N=15$). The muscle mass and mean fibre length were 5.2 ± 0.3 mg ($N=15$) and 9.1 ± 0.1 mm ($N=15$), respectively. The mean isometric stress was 342.5 ± 8.3 kN m⁻² ($N=15$), which is somewhat higher than has been previously reported (211–269 kN m⁻², e.g. Luff, 1981; Brooks *et al.* 1990; James *et al.* 1995; Askew and Marsh, 1997). The explanation for this discrepancy is unclear, although it is possible that there were differences in architecture between these muscles and those used in a previous study using the same age, sex and strain of mouse (Askew and Marsh, 1997). The value of the ratio L_f/L_0 from this earlier study was used to estimate fibre length in the present investigation, and fibre length influences the calculation of cross-sectional area. However, these differences will not alter the conclusions of the paper. An isometric twitch:tetanus ratio of 0.11 was obtained. The latency between the stimulus and the start of force rise was 1.8 ms. The twitch kinetics were as follows: time to half-peak force, 4.5 ± 0.2 ms ($N=15$); time to peak force, 18.2 ± 0.6 ms ($N=15$); time from peak force to half-relaxation, 24.1 ± 0.7 ms ($N=15$); time from peak force to 90% relaxation, 29.3 ± 2.4 ms ($N=15$). Tetanic half-relaxation time was 37.1 ± 1.2 ms ($N=15$).

The isometric tetanic force varied considerably with starting length (Fig. 2). There was a range of starting lengths ($\pm 4.5\%$ L_0) across which force was approximately constant (at least $0.98P_0$), above and below this region force rapidly declined. The passive force was low at starting lengths below L_0 , but rapidly increased above L_0 , exceeding the active force at lengths above approximately $1.3L_0$ (Fig. 2).

The maximum shortening velocity (V_{\max}) estimated from the

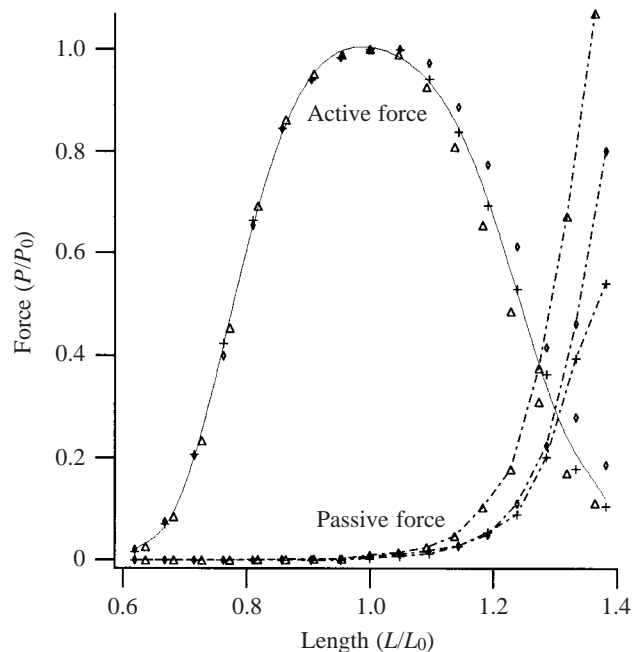


Fig. 2. The length–force relationship of three mouse soleus muscles as determined during tetanic stimulation. Both active and passive force are shown. Force is expressed relative to maximum isometric stress P_0 , and muscle length L is expressed relative to L_0 , the optimal length for the production of isometric tetani.

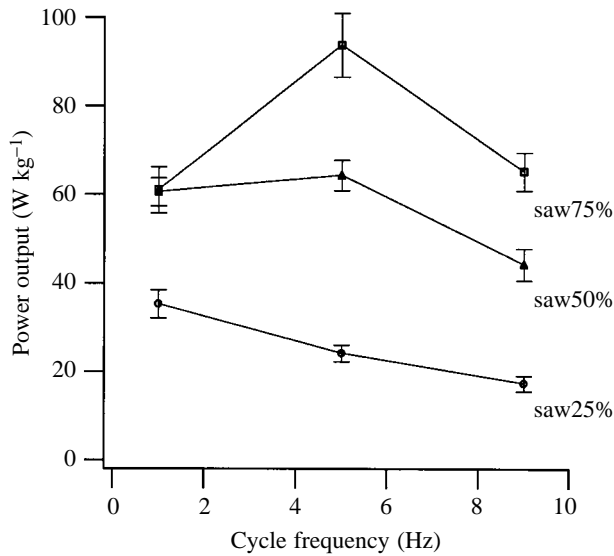


Fig. 3. The effects of cycle frequency and strain trajectory on power output. Data are shown for cycles in which the fraction of the cycle spent shortening was 25 % (saw25%), 50 % (saw50%) and 75 % (saw75%) (see Materials and methods). Values are means \pm S.E.M., $N=5-6$.

force-velocity relationship was $6.4 \pm 0.2 L s^{-1}$ ($N=15$). There was no statistically significant relationship between mouse age and either V_{\max} (correlation coefficient, $r=0.02$) or the shape of the force-velocity curve as indicated by the power ratio (correlation coefficient, $r<0.01$) over the age range studied. Values for the constants in the Marsh-Bennett force-velocity equation were $A=0.11 \pm 0.01$ ($N=15$), $B=0.59 \pm 0.06$ ($N=15$) and $C=1.01 \pm 0.12$ ($N=15$). The power ratio ($\dot{W}_{\max}/P_0 V_{\max}$) was 0.08 ± 0.003 ($N=15$), where \dot{W}_{\max} is the maximum isotonic power output. The maximum isotonic power output, $167.4 \pm 9.1 W kg^{-1}$ ($N=15$), was obtained at a force and velocity corresponding to 0.36 ± 0.01 ($N=15$) and 0.22 ± 0.01 ($N=15$) of the maximum isometric force (P_0) and maximum shortening velocity (V_{\max}), respectively. The maximum isotonic power output was higher than has been previously measured on the mouse soleus (Luff, 1981; Askew and Marsh, 1997), which is consistent with our higher isometric stress. The value of V_{\max} was similar to that reported for the same strain, sex and age of mouse (Askew and Marsh, 1997).

Power output during cyclical contractions

The maximum net power output of the muscles ranged from $17.3 \pm 1.7 W kg^{-1}$ ($N=5$), obtained using a 9 Hz saw25% strain trajectory, to $93.7 \pm 7.2 W kg^{-1}$ ($N=5$), using a 5 Hz saw75% strain trajectory (Fig. 3). At a given cycle frequency, the net power output increased with increasing proportion of the cycle spent shortening, except for 1 Hz where the maximum net power output during saw50% cycles was approximately equal to that developed during saw75% cycles. This influence of strain trajectory on power output has been discussed previously for mouse soleus and extensor digitorum longus muscles (Askew and Marsh, 1997).

Table 1. Maximum net power output and optimal V/V_{\max} for different strain trajectories

Cycle frequency (Hz)	Strain trajectory	Maximum power output ($W kg^{-1}$)	Optimal V/V_{\max}
1	Saw25%	35.3 ± 3.2 (5)	0.15
1	Saw50%	60.7 ± 3.2 (5)	0.10
1	Saw75%	61.0 ± 5.2 (5)	0.075
5	Saw25%	24.1 ± 1.9 (5)	0.25
5	Saw50%	64.4 ± 3.5 (5)	0.25
5	Saw75%	93.7 ± 7.2 (5)	0.20
9	Saw25%	17.3 ± 1.7 (5)	0.30
9	Saw50%	44.3 ± 3.5 (5)	0.25
9	Saw75%	65.2 ± 4.3 (6)	0.20

V , shortening velocity; V_{\max} , maximum shortening velocity. Values for power output are means \pm S.E.M. (N).

For a given cycle frequency and strain trajectory, there was an optimal V/V_{\max} at which the net power output was maximized (Fig. 4). The optimal V/V_{\max} increased with increasing cycle frequency (for a given strain trajectory) and decreased as the proportion of the cycle spent shortening increased (for a given cycle frequency) (Table 1; Fig. 4). For example, the optimal V/V_{\max} ranged from 0.075 at 1 Hz, saw75%, to 0.30 at 9 Hz, saw25% (Table 1; Fig. 4).

Discussion

Optimal V/V_{\max} during cyclical contractions

Numerous workers, starting with A. V. Hill (e.g. Hill, 1950; Goldspink, 1977; Rome, 1994), have predicted that skeletal muscle operating to produce power *in vivo* should operate at a relative shortening velocity (V/V_{\max}) that matches that at which the muscle can produce peak isotonic (or isovelocity) power. Testing this prediction is complicated by the fact that many muscles *in vivo* do not shorten at a constant velocity (Marsh *et al.* 1992; Marsh, 1994). However, some measurements of muscles operating in repeated cycles of contraction appear to agree with the prediction, at least approximately (Rome *et al.* 1988, 1992). From the data presented here, we suggest that this simple prediction based on the isotonic force-velocity curve (Fig. 1) may not hold for cyclical contractions under varied conditions.

Our results clearly show that the optimal V/V_{\max} is not constant during cyclical contractions, but depends on the conditions under which the muscle contracts. For simplicity, we used a sawtooth strain trajectory that holds V constant during shortening and we optimized stimulus phase and duration to produce the maximum net power output at each shortening velocity. We found that the optimal V/V_{\max} for mouse soleus muscle increased with increasing cycle frequency and decreased as the proportion of the cycle spent shortening increased (Fig. 4; Table 1). Over the range of conditions that we tested, the optimal V/V_{\max} varied almost fourfold, from 0.075 to 0.30. Maximum isotonic power

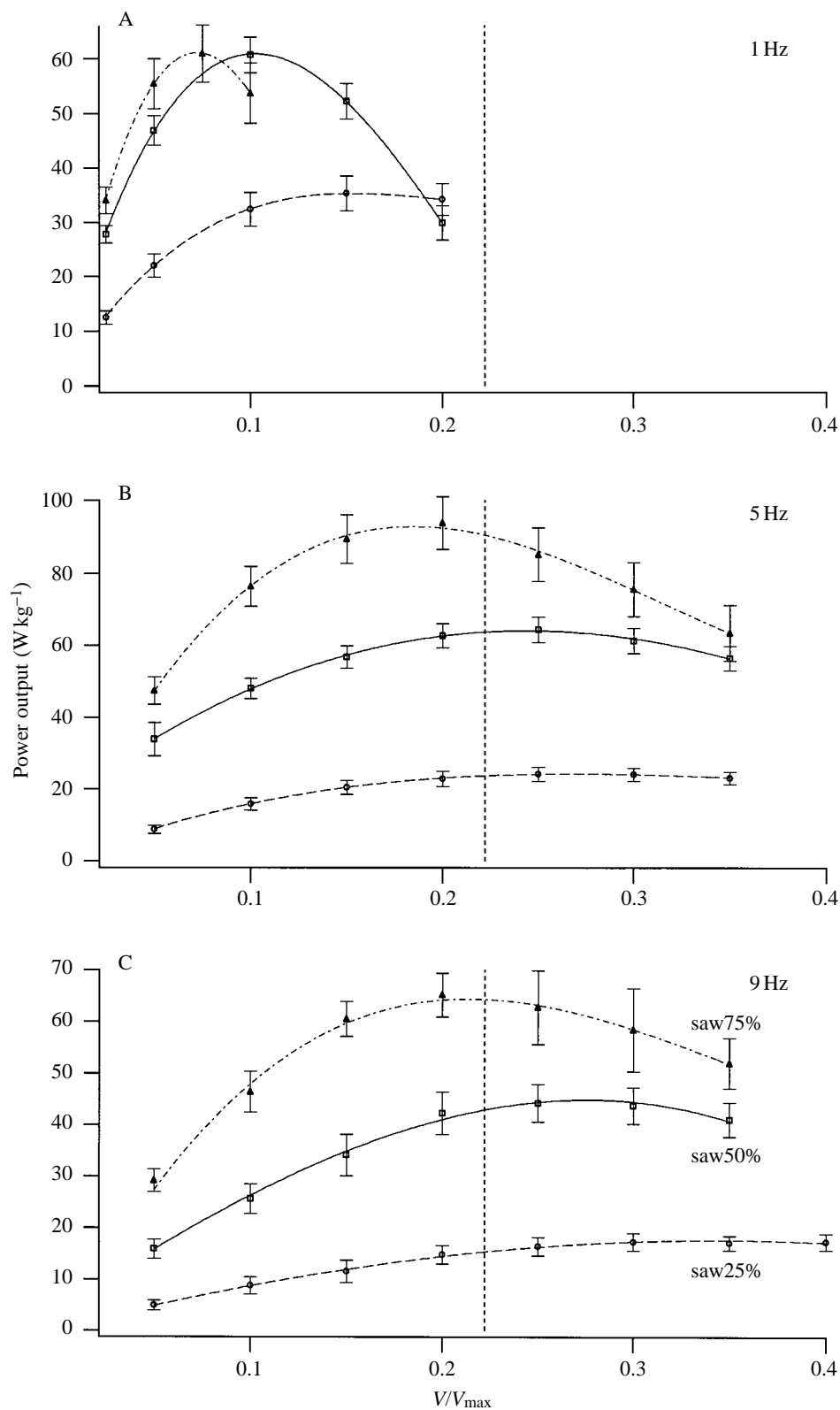


Fig. 4. Mechanical power output at cycle frequencies of 1 Hz (A), 5 Hz (B) and 9 Hz (C), using different strain trajectories, are plotted against relative shortening velocity V/V_{\max} . The value of V/V_{\max} that yielded peak power output on the basis of the force-velocity relationship is illustrated by the vertical dashed line. Fourth-order polynomials have been fitted to the data for each strain trajectory. Data represent mean \pm S.E.M. for five muscles (except for 9 Hz saw75%, where six muscles were used). The symbols and lines used to indicate the different strain trajectories are labelled in C. V , shortening velocity; V_{\max} , maximum shortening velocity.

occurred at a V/V_{\max} of 0.22. These results could be important *in vivo* for muscles that operate over a substantial range of frequencies; for example, the muscles of fish. In fish, the slow red muscles are first recruited at slow swimming speeds and

power the animal over a substantial range of frequencies (Bone, 1966; Davison *et al.* 1976; Rome *et al.* 1984; Jayne and Lauder, 1994). As the animal swims faster, these muscles continue to be active along with the fast white muscles to

power burst swimming. The white muscles are also active over a range of frequencies as the animal swims faster above its critical speed (Bone, 1966; Davison *et al.* 1976; Rome *et al.* 1984; Jayne and Lauder, 1994). Note that, in this example, the muscles perform symmetrical cycles of contraction. The optimal V/V_{\max} increases with cycle frequency in symmetrical as well as asymmetrical cycles (Fig. 4).

The variation in optimal V/V_{\max} with cycle frequency and shape results from the influences of other factors that help determine the power output during cyclical contractions. These effects can be described most effectively after describing a simple model of muscle function during cyclical contractions.

Modelling force during cyclical contractions on the basis of the muscle's intrinsic properties

There have been a number of attempts to relate the intrinsic properties of skeletal muscle to *in vivo* performance (e.g. van Leeuwen *et al.* 1990; Askew, 1995). These models assume that the mechanical properties measured under steady-state conditions apply during cyclical contractions. We similarly based a model on the measured steady-state properties of soleus muscle. Using parameters normalized relative to P_0 , it was assumed that the total force F_{Total} generated during a cyclical contraction was the product of three forces. (i) The force generated at a given velocity based on the force–velocity relationship, F_{PV} . We used our force–velocity data for shortening velocities and used an equation from Otten (1988) for lengthening velocities. (ii) The force generated at a given length based on the length–force relationship, F_{LF} (Fig. 2). (iii) The mechanical activation based on the time course of force during an isometric tetanus, F_{ACT} . Thus, we obtained the equation:

$$F_{\text{Total}} = F_{\text{PV}} \times F_{\text{LF}} \times F_{\text{ACT}}. \quad (2)$$

The third factor in equation 2 deserves special comment here and is discussed further below. We have referred to this term as the ‘mechanical activation’ and have defined it in terms of the development and relaxation of force that occurs under isometric conditions. During force development, the mechanical activation term is determined by the Ca^{2+} binding events and by subsequent events related to the establishment of a steady state in cycling crossbridges (Bagni *et al.* 1988). Current evidence suggests that the Ca^{2+} release is rapid and does not limit the rate of activation (Caputo *et al.* 1994). The effect of diffusive limitations is not entirely clear (Holly and Poledna, 1989; Poledna and Simurdova, 1992). A considerable portion of the delay in force development is due to crossbridge events (Bagni *et al.* 1988). For convenience, we refer below to all of these processes that lead to changes in the ability of the muscle to produce force and to shorten as ‘activation’. During the decline in force (relaxation), the events that underlie the mechanical activation term include Ca^{2+} removal from the sarcoplasm, Ca^{2+} dissociation from troponin (a process that is sensitive to the mechanical state of the muscle, see below) and crossbridge release. For convenience, we refer to these events as ‘deactivation’ and discuss the mechanical events that influence the ‘rate of deactivation’ after accounting for length–force and

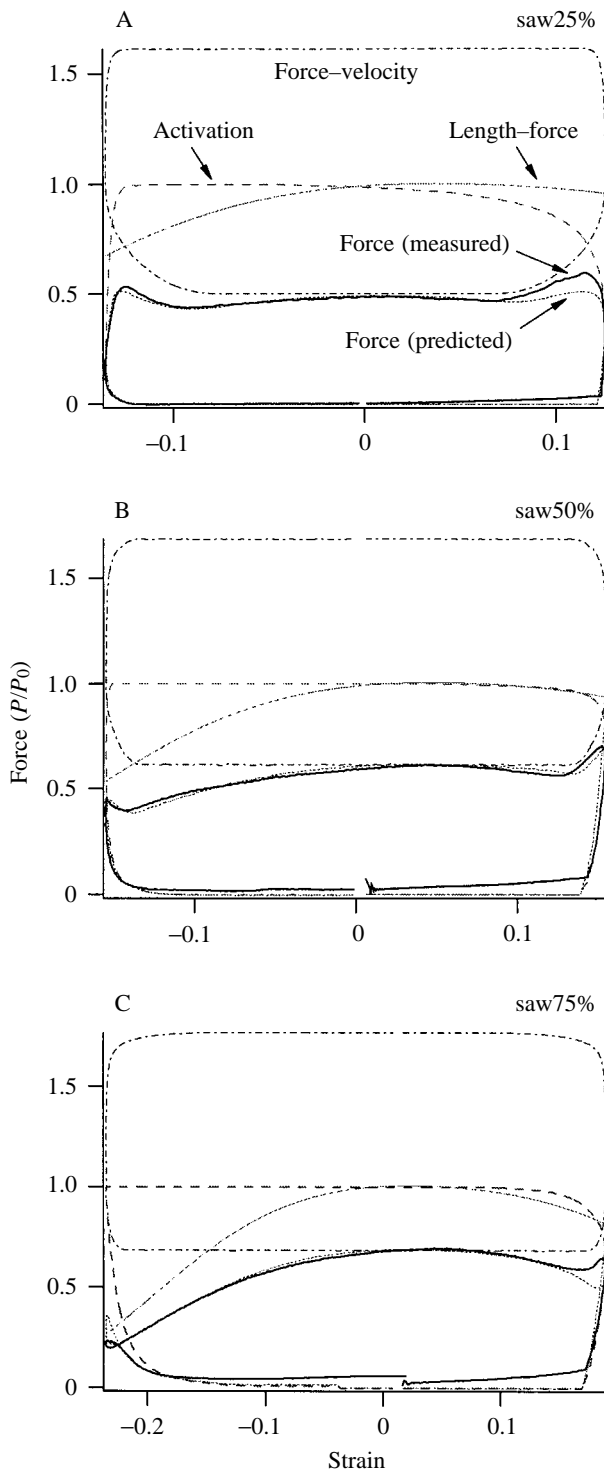
force–velocity effects. Using the term ‘deactivation’ to describe events that occur after the stimulation has ended is potentially confusing because this term is also used to describe events that occur in skeletal muscle during continuous stimulation, e.g. shortening-dependent deactivation, and these events probably rely on separate mechanisms (see below). However, in cardiac muscle, because of the inherently phasic contraction pattern, shortening-dependent deactivation refers to events following the single stimulus (Landesberg, 1996). In our opinion, using the alternative term ‘relaxation’ for events occurring during cyclical contractions is not without problems, because it is defined in isometric contractions by measuring force, and force during cyclical contractions is determined by multiple factors, including length–force and force–velocity effects.

At low cycle frequencies, equation 2 accurately predicted the force generated during cyclical contractions (Fig. 5). The only noticeable discrepancy was at the start of shortening, when the predicted force was slightly lower (approximately 10%) than that observed during experimental work loops. However, at high cycle frequencies, large discrepancies were observed (Fig. 6). Shortly after the onset of stimulation, force started to rise, and the discrepancy between the calculated and experimental forces was minimal as the muscle was stretched. However, as stretching slowed and the muscle started to shorten, the calculated force was much lower than that actually measured (Fig. 6C,G). Towards the end of shortening, the predicted and measured forces converged, only to diverge again as the muscle started to deactivate. Equation 2 overestimated force throughout the end of shortening and into the lengthening phase (Fig. 6C,G). The work loops calculated in this way were unrealistic and underestimated the net power output considerably (Fig. 6B,F). The calculated positive work was lower and the negative work was higher than those measured experimentally. The potential mechanisms underlying these results are described in the following sections.

Effects of the length–force relationship on the optimal V/V_{\max}

The length at which a muscle generates its maximum isometric stress is often defined as L_0 . This same stress can be generated over a range of lengths a few percent above and below L_0 (Fig. 2; Woledge *et al.* 1985). At lengths above and below this plateau region, force declines. The mechanical causes for this relationship are related to the degree of overlap between the actin and myosin filaments, i.e. the number of crossbridges that can be formed (Gordon *et al.* 1966). The distinct regions of the length–force curve observed in single-fibre studies are less sharply defined in our whole muscles (e.g. Fig. 2), presumably because of small differences in the relative length of different fibres at a given muscle length.

At low cycle frequencies and strain trajectories, where the proportion of the cycle spent shortening was greater than that spent lengthening, the length–force relationship resulted in a shift in the optimal V/V_{\max} below that yielding the maximum isotonic power output (Fig. 4). For a given strain trajectory and V/V_{\max} , strain amplitude decreases with increasing cycle frequency (for example, a V/V_{\max} of 0.2 is obtained at a strain



amplitude of approximately $\pm 16.1\%$ at 1 Hz and at $\pm 1.8\%$ at 9 Hz, for a saw50% strain trajectory). At strain amplitudes greater than $\pm 3\%$, the length-force relationship will play a role in reducing the force obtained during shortening. This dramatic reduction in force with increasing strain primarily causes the reduction in the optimal V/V_{\max} at low cycle frequencies and also at higher cycle frequencies, when the proportion of time spent shortening is high. Weis-Fogh and Alexander (1977), using a

Fig. 5. Examples of work loops for mouse soleus at 1 Hz during (A) saw25%, (B) saw50% and (C) saw75% length trajectories (see Materials and methods). Predicted work loops (dotted line) have been calculated on the basis of the force-velocity relationship, the length-force relationship and the kinetics of activation and deactivation based upon isometric measurements using equation 2. The force as a function of strain is plotted on the basis of each of these relationships. The force-velocity and the activation relationships are different during shortening and lengthening and thus form loops. The activation loop is traced anticlockwise, whereas the force-velocity loop is clockwise because greater force is predicted during lengthening. The experimentally obtained work loop is shown with a solid black line. The experimental and predicted work loops are anticlockwise and represent net positive work. Force is expressed relative maximum isometric stress P_0 .

simple mathematical model of muscle contraction including force-velocity and length-force effects (but not activation events), arrived at the same conclusion, that the optimal V/V_{\max} ($\eta \epsilon_{\max}/\dot{\epsilon}_0$ in Weis-Fogh and Alexander, 1977) decreased with decreasing cycle frequency.

Effects of the kinetics of activation and deactivation on the optimal V/V_{\max}

At high cycle frequencies and also during asymmetrical cycles dominated by lengthening at lower frequencies, where the strain amplitude is low, the effects of the length-force relationship are necessarily small. Under these conditions, the optimal V/V_{\max} is actually higher than that predicted from the force-velocity relationship (Fig. 4). We believe that this results from changes in the kinetics of activation and deactivation at different rates of lengthening and shortening. Activation and deactivation (see above for definitions) represent an increasing proportion of the duty cycle as both cycle frequency and lengthening duration increase. Thus, any changes in the rates of activation and deactivation will have greatest effects on work during such contractions.

The large discrepancies that we observed at high cycle frequencies between the force calculated from equation 2 and that measured provide evidence for changes in the rates of activation and deactivation. To estimate the changes in the kinetics of activation and deactivation during cyclical contractions compared with isometric conditions, we calculated an apparent mechanical activation component (f_{act}). We made the assumption that the force-velocity relationship and length-force relationship were applicable at all cycle frequencies. Any difference between the observed force and that predicted from these two relationships was ascribed to activation. The apparent activation component was thus calculated by dividing the force obtained experimentally (F) by that predicted from the force-velocity and length-force relationships:

$$f_{\text{act}} = \frac{F}{F_{\text{PV}} \times F_{\text{LF}}} \quad (3)$$

At high frequencies, the measured force early in shortening was much higher than expected from isometric activation

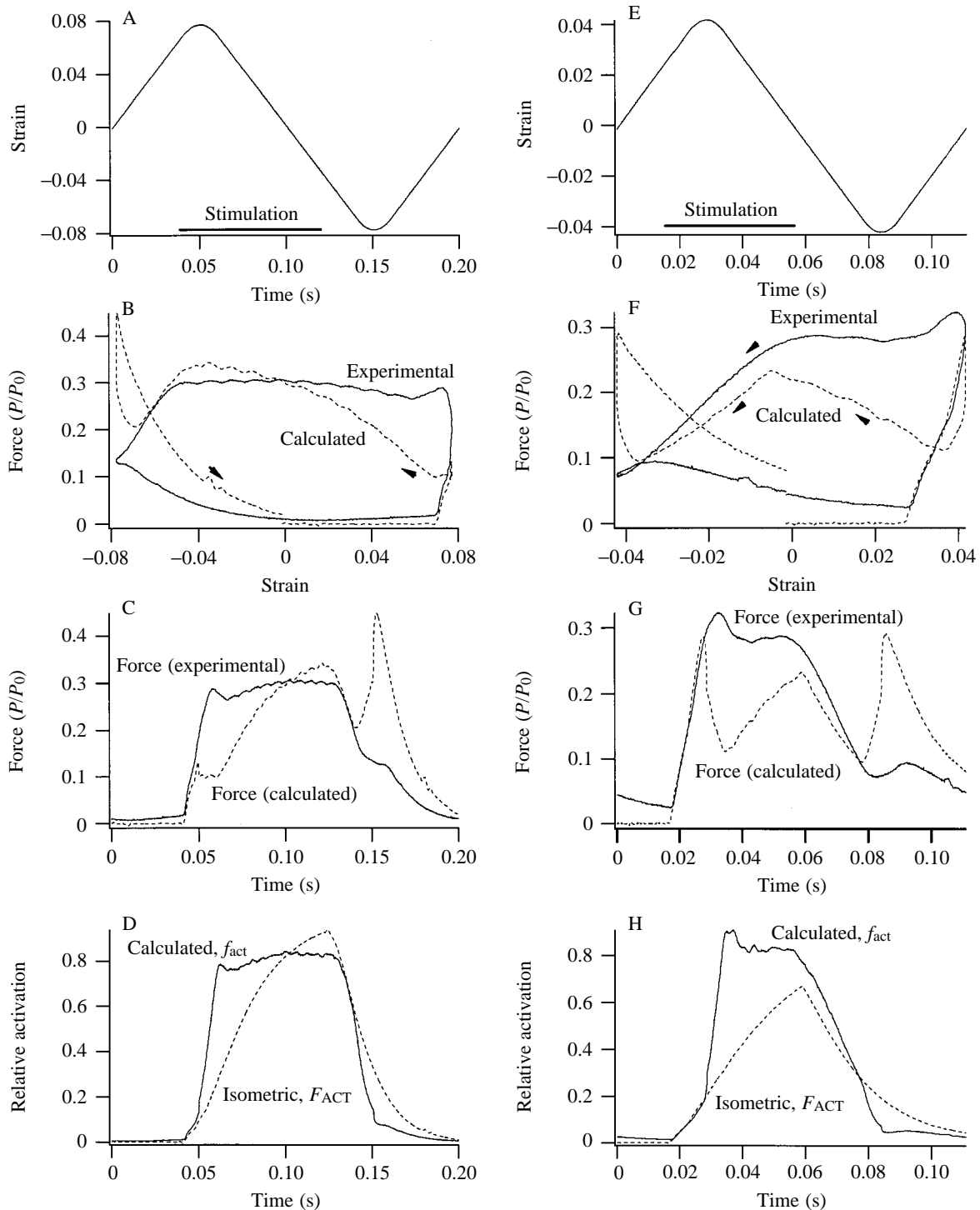


Fig. 6. Measured and predicted forces during cyclical contractions at 5 Hz saw50% (A–D) and 9 Hz saw50% (E–H) (see Materials and methods). (A,E) The strain and timing of stimulation. (B,F) Experimental and predicted (calculated) work loops. (C,G) The measured force and that calculated from the muscle's intrinsic properties (equation 2). (D,H) The mechanical activation force (F_{ACT}) predicted from the isometric tetanus on the basis of the timing of stimulation. F_{ACT} is the activation curve used in equation 2 to predict force. Also shown is the apparent mechanical activation force (f_{act}) from equation 3, which represents the activation that would be required to explain the discrepancy between the modelled and the measured forces. Force is expressed relative maximum isometric stress P_0 . Arrowheads indicate the direction of work loops.

kinetics and, conversely, the measured forces late in shortening and during lengthening were much lower than predicted

(Fig. 6C,G). Therefore, using equation 3, we estimated that during cyclical contractions the apparent activation rose and

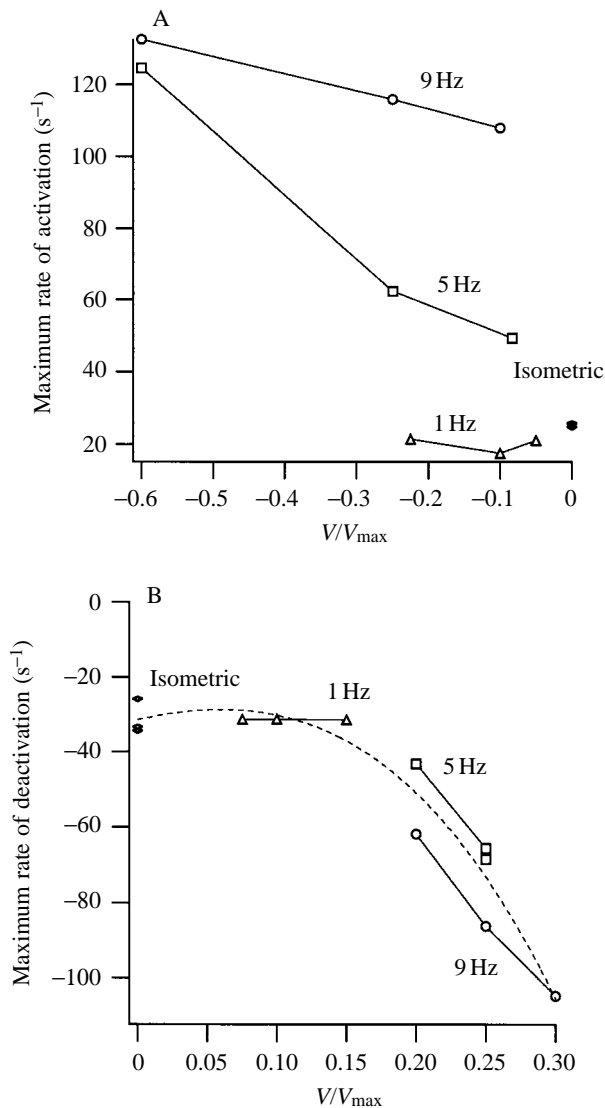


Fig. 7. Maximum apparent rate of activation (A) and deactivation (B) relative to full activation plotted against lengthening velocity and shortening velocity, respectively. These plots are based on the differential of the predicted apparent mechanical activation component (f_{act}) calculated using equation 3 for optimized work loops at the relative shortening velocity V/V_{max} for maximum net power output for each cycle frequency and strain trajectory studied.

declined more rapidly than activation as predicted from isometric conditions (Fig. 6D,H). This method was used to determine the time course of f_{act} for each of the cycle frequencies and strain trajectories examined in the study. The resulting f_{act} curves were used to estimate the maximum rate of apparent activation and deactivation by differentiating f_{act} with respect to time (Fig. 7). These rates are expressed as multiples of full activation per second.

The predicted rate of activation required to explain the experimental data increased with both cycle frequency and the velocity of stretch (Fig. 7A). At a cycle frequency of 1 Hz, the rate was similar to that measured during isometric tetani and

was independent of stretch velocity up to approximately $-0.2V/V_{max}$. At 5 and 9 Hz, the rate of apparent activation increased with stretch velocity and was always higher at 9 Hz than at 5 Hz. The increase in the rate of activation with increasing cycle frequency at equal stretch velocities could be related to the amplitude of the active stretch. If this is the case, then smaller stretches are actually more effective than larger ones as strain during these optimized cycles decreases with increasing frequency. Surprisingly, the apparent activation diverges most sharply from the isometric values after most of the stretch has been completed, but this effect requires further investigations that include the effects of elasticity.

Our model does not include the effects of series elasticity, which should be included in future models (Curtin *et al.* 1998), but elastic effects are not able to explain the observed effects of stretch. When the muscle is activated during lengthening, the force developed will stretch series elastic structures, such as the tendon, in proportion to the force developed. During stretch, this effect would reduce the velocity of stretch of the contractile elements and thus reduce the observed force below that predicted by our model (Curtin *et al.* 1998). Actually, force during the stretching phase agreed well with our model. Inclusion of significant elasticity in the model would thus require that the rate of activation during the stretching phase be greater than we have predicted on the basis of our current model. Therefore, elastic effects might eliminate the discontinuity in our predictions of apparent activation (Fig. 6D,H) by shifting more of the effect to the stretching phase, but these effects would not influence our conclusion that stretching enhances activation. Decreases in muscle force during subsequent shortening would allow the series elastic elements to shorten, thus decreasing the velocity of filament sliding for a given rate of muscle shortening. This elastic recoil would result in a higher force than predicted by our model. Actually, elasticity can account for little of the discrepancy in force and work during shortening because in many cases the force drops little during shortening until deactivation begins (Fig. 6C,G). During the major drop in force at the end of shortening, when elastic recoil is expected to take place, the measured force is actually considerably smaller than the predictions of the model. Part of the enhancement of force at the start of shortening could be due to elastic strain energy released from the tendon. However, the effects of elastic strain energy release during the initial shortening phase would be to increase the instantaneous power output, but not the net work or net power output, because negative work is performed on the elastic elements during active lengthening. In contrast, our results show that net work is considerably increased by the apparent increase in the rate of activation (Fig. 6B,F).

We also found that the predicted maximum rate of deactivation increased with increasing cycle frequency and increasing V/V_{max} during shortening and this enhanced deactivation was essential to maintaining power output at high frequencies (Fig. 6). To illustrate this effect clearly, we have plotted data in which frequency, stimulus phase and stimulus duration were held constant but V/V_{max} was varied by changing

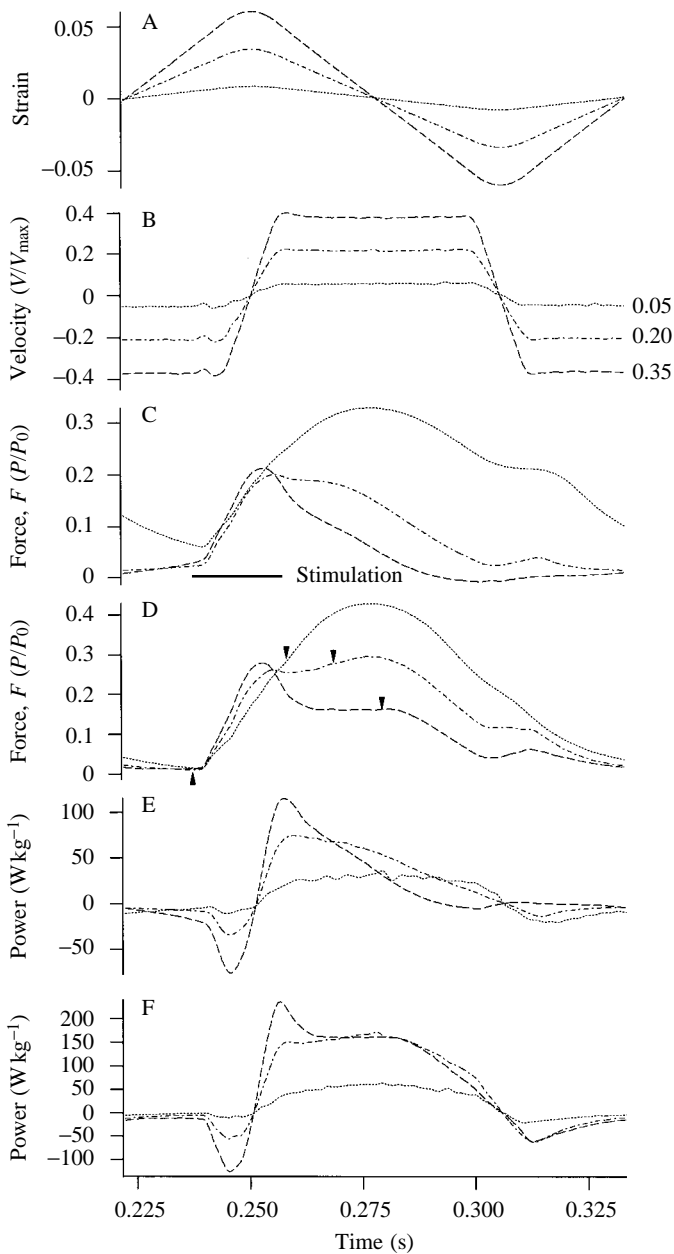


Fig. 8. The third cycle from experiments with a mouse soleus muscle subjected to 9 Hz cycles and a saw50% strain trajectory (see Materials and methods) at three different values (0.05, 0.20 and 0.35) of relative shortening velocity V/V_{\max} . (A) The strain to which the muscle was subjected; the corresponding velocity is given in B. (C) The force produced at each strain using a constant stimulation phase of 12 ms before the start of shortening (-40°) and a stimulation duration of 20 ms. The stimulation period is represented by the bar below the force records. (D) The force produced using optimal stimulation parameters for each of the strains illustrated in A. In each case, a phase of -40° was used (marked by an upward-pointing arrowhead), but the stimulation duration ranged from 20 ms (for $V/V_{\max}=0.05$) to 40 ms (for $V/V_{\max}=0.35$). The end of stimulation is marked with a downward-pointing arrowhead. The power output corresponding to each of the force traces in C and D is shown in E and F, respectively. Force is expressed relative maximum isometric stress P_0 .

strain (Fig. 8C,E). These data indicate that the time required for deactivation decreased with increasing V/V_{\max} . In cycles optimized for net power output, reducing the time taken for the muscle to relax at a higher V/V_{\max} coupled with a lower shortening force (force-velocity effects) allows the muscle to be stimulated for longer and to remain more fully activated later in the shortening period (Figs 6, 8D,F). The effect of shortening velocity on deactivation resulted in a shift in the optimal V/V_{\max} at high cycle frequencies to a value above that predicted by the force-velocity relationship (Fig. 4). More rapid relaxation of force increases the positive work performed during shortening without increasing the negative work during lengthening. Thus, the net power output is increased.

As with the activation events discussed above, differentiating the curve resulting from equation 3 resulted in a prediction of the maximum rate of apparent deactivation required to account for the observed force during optimized cycles. We found that the rate of deactivation was velocity-dependent. The rate of deactivation at low values of V/V_{\max} during 1 Hz cycles was essentially the same as during an isometric tetanus (Fig. 7B), as would be predicted from the high degree of similarity between experimental and calculated work loops (Fig. 5). At values of V/V_{\max} above 0.15, using frequencies of 5 and 9 Hz, the rate of deactivation increased. These changes appear to be related to velocity and not to the amount of shortening. The rate of deactivation is actually slightly faster at the same V/V_{\max} during 9 Hz cycles than during 5 Hz cycles that have higher strains.

Other workers have found that length changes produce changes in activation and deactivation during continuous stimulation, but the relevance of many of these studies to cyclical contractions with phasic stimulation is unclear. Active lengthening of a fully stimulated muscle results in an enhancement of force. The increase in force is separable into an effect during stretch (the negative force-velocity effect) and a prolonged effect sometimes termed stretch enhancement (Edman *et al.* 1978; Takarada *et al.* 1997b). The mechanism for the effects of stretch on fully stimulated muscle and its significance for muscle performance are controversial (Cavagna *et al.* 1994; Edman and Tsuchiya, 1996; Edman, 1997). In insect asynchronous muscles, stretch activation plays an essential role in power generation (Pringle, 1978), and this property may be general, arising from the non-linear properties of the crossbridges (Thomas and Thornhill, 1996). Shortening of a fully stimulated muscle causes a reduction in the ability of the muscle to produce force, an effect that has been termed a force deficit or depression (Edman, 1980; Granzier and Pollack, 1989). The magnitude of this effect is negatively correlated with shortening velocity and positively correlated with the amount of work done (Granzier and Pollack, 1989).

Much less effort has been directed towards understanding the mechanisms involved when length changes are in phase with the beginning and end of stimulation. Investigators have often assumed that the effects of stretch and shortening that occur in fully activated muscle also apply in partially activated muscle (Josephson and Stokes, 1989; Altringham *et al.* 1993;

Takarada *et al.* 1997a). However, the mechanisms may be quite distinct (Edman *et al.* 1993).

Earlier work of A. V. Hill and others examined the effects of stretch in the period immediately following stimulation (Hill, 1970). These experiments make it clear that a muscle stretched early in the stimulation period reaches P_0 much more quickly than the same muscle held isometric. Of course, the original interpretation of these experiments exclusively in terms of stretching the series elastic elements is no longer tenable, but the underlying mechanism has never been fully elucidated. Possibly, the effect is mediated *via* an influence on the rate of development of the steady-state level of crossbridge attachment. Because in most models of crossbridge function the rate of detachment is position-dependent (Huxley, 1957; Eisenberg *et al.* 1980), bridges stretched during the activation phase will be held in a zone of low detachment rate. Decreasing the detachment rate while keeping the attachment rate high would enhance the rate of increase in the net number of attached bridges. This increase in net attachment would be particularly true in comparison with isometric contractions that actually involve some internal shortening of the contractile elements at the expense of series elastic elements. Whatever the mechanism, the data presented here make it clear that at high contractile frequencies enhanced activation with stretch can result in a substantial augmentation of work output during subsequent shortening (Fig. 6).

A mechanism for the velocity-dependent deactivation noted in the present study can be postulated with somewhat more certainty than the effects of stretch. First, it should be noted that the effects of shortening *per se* on the number of attached crossbridges is expected to be modest. The highest velocities we used ($0.4V_{\max}$) would be expected to decrease the number of crossbridges by approximately 40% compared with isometric conditions (Ford *et al.* 1985). This effect is included in our model as part of the force-velocity effect during shortening. The dramatically lower than predicted forces at the end of shortening (Figs 6, 8) can only be explained if the number of crossbridges is substantially reduced below that predicted from isometric deactivation. The effect of shortening during isometric relaxation has been examined by Gordon and Ridgway (1987) and Caputo *et al.* (1994). They measured the effects of shortening on the myofibrillar Ca^{2+} concentration, as estimated using Ca^{2+} -specific photoproteins. Shortening causes extra Ca^{2+} to be released from the Ca^{2+} -binding proteins (Gordon and Ridgway, 1987; Caputo *et al.* 1994), with the amount of Ca^{2+} released being proportional to the rate of shortening and inversely related to the number of attached crossbridges (Gordon and Ridgway, 1987). Apparently, filament movement decreases the affinity of troponin for tropomyosin, an effect that can also explain the transition from the linear to the pseudo-exponential phase of relaxation during isometric tetani (Cannell, 1986; Caputo *et al.* 1994). Interestingly, according to Caputo *et al.* (1994), stretching the muscle in the period of linear relaxation does not cause the opposite effect to that of shortening. This result is intriguing because our results show that, at the turnaround between

muscle shortening and lengthening, there is very little increase in force (Fig. 6); instead, deactivation proceeds at a rapid rate. As pointed out above the effects seen here appear to be velocity-dependent and not shortening-dependent, but distinguishing these possibilities will require further experiments.

In conclusion, we have clearly shown that factors in addition to the force-velocity relationship are important in determining the optimal V/V_{\max} during cyclical contractions at different cycle frequencies and during different strain trajectories. A fourfold range of optimal V/V_{\max} was found over the range of conditions examined (Fig. 4). At low cycle frequencies and using strain trajectories in which the proportion of time spent shortening was greater than that spent lengthening, the reduction in work due to the effects of the length-force relationship at large strain amplitudes (Fig. 2) resulted in a reduction in the optimal V/V_{\max} below that predicted from the force-velocity relationship (Fig. 4). Conversely, at high cycle frequencies and using strain trajectories with brief shortening periods, the optimal V/V_{\max} was greater than that predicted from the force-velocity relationship. Velocity-dependent rates of activation and deactivation at high strain rates allowed more work to be performed during shortening without increasing the work during lengthening (Figs 7, 8). These effects account for the increase in optimal V/V_{\max} . Thus, for muscles that operate over a range of shortening velocities (e.g. fish red muscle) and/or strain trajectories, the force-velocity relationship alone cannot simply be used to estimate the optimal V/V_{\max} for power production.

A simple model based upon the force-velocity and length-force relationships and rates of force rise and relaxation determined from isometric tetani accurately predicted force during cyclical contractions at low cycle frequencies. However, at high cycle frequencies, changes in the kinetics of activation and deactivation caused large discrepancies between predicted and measured forces (Fig. 6). Similar models attempting to predict force during cyclical contractions on the basis of a muscle's intrinsic properties have fallen short of reproducing what actually occurs. The greatest discrepancy has been in predicting force during deactivation (Sandercock and Heckman, 1997; Curtin *et al.* 1998), but we also found differences during activation (Fig. 6). To develop such models further, a better quantitative understanding of the responses of partially activated muscle to length changes is required.

This work was supported by a grant from the NIH to R.L.M. (AR39318).

References

- ALTRINGHAM, J. D., WARDLE, C. S. AND SMITH, C. I. (1993). Myotomal muscle function at different locations in the body of a swimming fish. *J. exp. Biol.* **182**, 191–206.
- ASKEW, G. N. (1995). Mechanical properties of mammalian fast and slow muscles and the effects of training for potential use in cardiomyoplasty. PhD thesis, University of Leeds.

- ASKEW, G. N. AND MARSH, R. L. (1997). The effects of length trajectory on the mechanical power output of mouse skeletal muscles. *J. exp. Biol.* **200**, 3119–3131.
- BAGNI, M. A., CECCHI, G. AND SCHOENBERG, M. (1988). A model of force production that explains the lag between crossbridge attachment and force after electrical stimulation of striated muscle fibres. *Biophys. J.* **54**, 1105–1114.
- BONE, Q. (1966). On the function of the two types of myotomal muscle fibre in elasmobranch fish. *J. mar. biol. Ass. U.K.* **46**, 321–349.
- BROOKS, S. V., FAULKNER, J. A. AND MCCUBBREY, D. A. (1990). Power outputs of slow and fast skeletal muscles of mice. *J. appl. Physiol.* **68**, 1282–1285.
- CANNELL, M. B. (1986). Effect of tetanus duration on free calcium during the relaxation of frog skeletal muscle fibres. *J. Physiol., Lond.* **376**, 203–218.
- CAPUTO, C., EDMAN, K. A. P., LOU, F. AND SUN, Y.-B. (1994). Variation in myoplasmic Ca^{2+} concentration during contraction and relaxation studied by the indicator fluo-3 in frog muscle fibres. *J. Physiol., Lond.* **478**, 137–148.
- CAVAGNA, G. A., HEGLUND, N. C., HARRY, J. D. AND MANTOVANI, M. (1994). Storage and release of mechanical energy by contracting frog muscle fibres. *J. Physiol., Lond.* **481**, 689–708.
- CURTIN, N. A., GARDNER-MEDWIN, A. R. AND WOLEDGE, R. C. (1998). Predictions of the time course of force and power output by dogfish white muscle fibres during brief tetani. *J. exp. Biol.* **201**, 103–114.
- DAUT, J. AND ELZINGA, G. (1989). Substrate dependence of energy metabolism in isolated guinea-pig cardiac muscle: a microcalorimetric study. *J. Physiol., Lond.* **413**, 379–397.
- DAVISON, W., GOLDSPIK, G. AND JOHNSTON, I. A. (1976). Division of labour between fish myotomal muscles during swimming. *J. Physiol., Lond.* **263**, 185–186.
- EDMAN, K. A. P. (1980). Depression of mechanical performance by active shortening during twitch and tetanus of vertebrate muscle fibres. *Acta Physiol. Scand.* **109**, 15–26.
- EDMAN, K. A. P. (1997). Force enhancement by stretch. *J. appl. Biomech.* **13**, 432–436.
- EDMAN, K. A. P., CAPUTO, C. AND LOU, F. (1997). Depression of tetanic force induced by loaded shortening of frog muscle fibres. *J. Physiol., Lond.* **466**, 535–552.
- EDMAN, K. A. P., ELZINGA, G. AND NOBLE, M. I. M. (1978). Enhancement of mechanical performance by stretch during tetanic contractions of vertebrate skeletal muscle fibres. *J. Physiol., Lond.* **281**, 139–155.
- EDMAN, K. A. P. AND TSUCHIYA, T. (1996). Strain of passive elements during force enhancement by stretch in frog muscle fibres. *J. Physiol., Lond.* **490**, 191–205.
- EISENBERG, E., HILL, T. L. AND CHEN, Y.-D. (1980). Crossbridge model of muscle contraction. *Biophys. J.* **29**, 195–226.
- FORD, L. E., HUXLEY, A. F. AND SIMMONS, R. M. (1977). Tension responses to sudden length change in stimulated frog muscle fibres near slack length. *J. Physiol., Lond.* **269**, 441–515.
- FORD, L. E., HUXLEY, A. F. AND SIMMONS, R. M. (1985). Tension transients during steady shortening of frog muscle fibres. *J. Physiol., Lond.* **361**, 131–150.
- GIRGENRATH, M. AND MARSH, R. L. (1997). *In vivo* performance of trunk muscles in tree frogs during calling. *J. exp. Biol.* **200**, 3101–3108.
- GOLDSPIK, G. (1977). Mechanics and energetics of muscle in different animals of different sizes, with particular reference to the muscle fibre composition of vertebrate muscle. In *Scale Effects in Animal Locomotion* (ed. T. J. Pedley), pp. 37–55. London, New York: Academic Press.
- GORDON, A. M., HUXLEY, A. F. AND JULIAN, F. J. (1966). The variation in isometric tension with sarcomere length in vertebrate muscle fibres. *J. Physiol., Lond.* **184**, 170–192.
- GORDON, A. M. AND RIDGWAY, E. B. (1987). Extra calcium on shortening in barnacle muscle: Is the decrease in calcium binding related to decreased crossbridge attachment, force, or length? *J. gen. Physiol.* **90**, 321–340.
- GRANZIER, H. L. M. AND POLLACK, G. H. (1989). Effect of active pre-shortening on isometric and isotonic performance of single muscle fibres. *J. Physiol., Lond.* **415**, 299–327.
- HILL, A. V. (1950). The dimensions of animals and their muscular dynamics. *Sci. Prog.* **38**, 209–230.
- HILL, A. V. (1970). *First and Last Experiments in Muscle Mechanics*. Cambridge: Cambridge University Press.
- HOLLY, M. AND POLEDNA, J. (1989). Model of calcium diffusion, binding and membrane transport in the sarcomere of frog skeletal muscle. *Gen. Physiol. Biophys.* **8**, 539–553.
- HUXLEY, A. F. (1957). Muscle structure and theories of contraction. *Prog. biophys. Chem.* **7**, 255–318.
- JAMES, R. S., ALTRINGHAM, J. D. AND GOLDSPIK, D. F. (1995). The mechanical properties of fast and slow skeletal muscles in relation to their locomotory function. *J. exp. Biol.* **198**, 491–502.
- JAYNE, B. C. AND LAUDER, G. V. (1994). How swimming fish use slow and fast muscle fibres: implications for models of vertebrate fibre recruitment. *J. comp. Physiol. A* **175**, 123–131.
- JOSEPHSON, R. K. (1985). Mechanical power output from striated muscle during cyclical contractions. *J. exp. Biol.* **114**, 493–512.
- JOSEPHSON, R. K. (1993). Contraction dynamics and power output of skeletal muscle. *A. Rev. Physiol.* **55**, 527–546.
- JOSEPHSON, R. K. AND STOKES, D. R. (1989). Strain, muscle length and work output in a crab muscle. *J. exp. Biol.* **145**, 45–61.
- LANDESBURG, A. (1996). End-systolic pressure–volume relationship and intracellular control of contraction. *Am. J. Physiol.* **270**, H338–H349.
- LUFF, A. R. (1981). Dynamic properties of the inferior rectus, extensor digitorum longus, diaphragm and soleus muscles of the mouse. *J. Physiol., Lond.* **313**, 161–171.
- LUTZ, G. J. AND ROME, L. C. (1996). Muscle function during jumping in frogs. II. Mechanical properties of muscle: implications for system design. *Am. J. Physiol.* **271**, C571–C578.
- MARSH, R. L. (1994). Jumping ability of anuran amphibians. In *The Advances in Veterinary Science and Comparative Medicine: Comparative Vertebrate Exercise Physiology* (ed. J. H. Jones), pp. 51–111. New York: Academic Press.
- MARSH, R. L. AND BENNETT, A. F. (1986). Thermal dependence of contractile properties of skeletal muscle from the lizard *Sceloporus occidentalis* with comments on methods for fitting and comparing force–velocity curves. *J. exp. Biol.* **126**, 63–77.
- MARSH, R. L., OLSON, J. M. AND GUZIK, S. K. (1992). Mechanical performance of scallop adductor muscle during swimming. *Nature* **357**, 411–413.
- MÉNDEZ, J. AND KEYS, A. (1960). Density and composition of mammalian muscle. *Metabolism* **9**, 184–188.
- OTTEN, E. (1988). A myocybernetic model of the jaw system of the rat. *J. Neurosci. Meth.* **21**, 287–302.
- POLEDNA, J. AND SIMURDOVA, A. (1992). Distribution of calcium during contraction and relaxation of crayfish skeletal muscle fibre. *Gen. Physiol. Biophys.* **11**, 427–439.

- PRINGLE, J. W. S. (1978). Stretch activation of muscle: function and mechanism. *Proc. R. Soc. Lond. B* **201**, 107–130.
- ROME, L. C. (1994). The mechanical design of the muscular system. In *The Advances in Veterinary Science and Comparative Medicine: Comparative Vertebrate Exercise Physiology* (ed. J. H. Jones), pp. 125–179. New York: Academic Press.
- ROME, L. C., FUNKE, R. P., ALEXANDER, R. MCN., LUTZ, G., ALDRIDGE, H. D., SCOTT, F. AND FREADMAN, M. (1988). Why animals have different muscle fibre types. *Nature* **355**, 824–827.
- ROME, L. C., LOUGHNA, P. T. AND GOLDSPIK, G. (1984). Muscle fibre activity in carp as a function of swimming speed and muscle temperature. *Am. J. Physiol.* **247**, R272–R279.
- ROME, L. C., SOSNICKI, A. AND CHOI, I. (1992). The influence of temperature on muscle function in the fast swimming scup. II. The mechanics of red muscle. *J. exp. Biol.* **163**, 281–295.
- SANDERCOCK, T. G. AND HECKMAN, C. J. (1997). Force from cat soleus muscle during imposed locomotor-like movements: experimental data *versus* Hill-type model predictions. *J. Neurophysiol.* **77**, 1538–1552.
- TAKARADA, Y., HIRANO, Y., ISHIGE, Y. AND ISHII, N. (1997a). Stretch-induced enhancement of mechanical power output in human multi-joint exercise with countermovement. *J. appl. Physiol.* **83**, 1749–1755.
- TAKARADA, Y., IWAMOTO, H., SUGI, H., HIRANO, Y. AND ISHII, N. (1997b). Stretch-induced enhancement of mechanical work production in frog single fibres and human muscle. *J. appl. Physiol.* **83**, 1741–1748.
- THOMAS, N. AND THORNHILL, R. A. (1996). Stretch activation and nonlinear elasticity of muscle crossbridges. *Biophys. J.* **70**, 2807–2818.
- VAN LEEUWEN, J. L., LANKHEET, M. J. M., AKSTER, H. A. AND OSSE, J. W. M. (1990). Function of red axial muscles of carp (*Cyprinus carpio*): recruitment and normalized power output during swimming in different modes. *J. Zool., Lond.* **220**, 123–145.
- WEIS-FOGH, T. AND ALEXANDER, R. MCN. (1977). The sustained power output from striated muscle. In *Scale Effects In Animal Locomotion* (ed. T. J. Pedley), pp. 511–525. London: Academic Press.
- WOLEDGE, R. C., CURTIN, N. A. AND HOMSHER, E. (1985). *Energetic Aspects of Muscle Contraction*. London: Academic Press.